

The Mechanical Properties of Insert-Molded Bimaterial Composites

C. W. EXTRAND and S. BHATT

Entegris
3500 Lyman Blvd.
Chaska, MN 55318

Bimaterial composite samples were constructed by injecting various polymers into a mold containing a fraction of a pre-molded specimen. The resulting series composites were tested in tension. Breaking stresses were independent of fractional length. Conversely, both elongation to break and apparent stiffness varied with fractional length. Although samples broke at or near the interface, adhesion was reasonably good, as indicated by transfer of material across interfaces.

INTRODUCTION

Insert molding involves injecting a polymer over another material (1, 2). This approach marries the best features of both materials and provides an economical method for producing higher performance products at a reduced cost. In some cases, it is a good alternative to polymer blends. An important consideration for any insert-molded product is the mechanical performance of the resulting bimaterial composite. However, little work has been published in this area (1), particularly for rigid thermoplastics. Recently, the mechanical properties (3) and interfacial adhesive strengths (4, 5) were investigated for poly(carbonate) (PC)/carbon fiber poly(etheretherketone) (C fiber PEEK) bimaterial composites.

In this study, the mechanical properties of a wide variety of rigid, bimaterial, polymer composites were examined. Series composite specimens were constructed by injecting unfilled and filled polymers into a mold containing a fractional piece of another polymer. The molten polymer locally melts the interface of the polymer insert to form a thermophysical bond. The resulting specimens were tested in tension and analyzed. The mechanical properties of the bimaterial composites were compared to their respective materials of construction.

ANALYSIS

Apparent Stresses and Strains

The stress field near the interface of bimaterial composites has been examined previously (6–12). For our work, the stress field in the immediate vicinity of the

interface was neglected. Our aim was to understand the apparent (or far-field) mechanical responses of bimaterial composites. The approach used to analyze our findings is given below (3).

Figure 1 shows a bimaterial composite tensile specimen. The specimen is comprised of two materials in series with tensile moduli of E_1 and E_2 , where $E_1 \leq E_2$. Both segments have the same cross-sectional area (A), but the relative length of each component (L_1 and L_2) can vary. Apparent tensile stress (σ) of monolithic or composite samples were calculated using the elongation force (F) divided by its initial or undeformed cross-sectional area (A) (13, 14),

$$\sigma = F/A. \quad (1)$$

From overall elongation (ΔL) of the specimen and its initial length (L), apparent strains (ε) were computed as

$$\varepsilon = \Delta L/L. \quad (2)$$

Tensile moduli (E) were calculated as apparent stress over apparent strain,

$$E = \sigma/\varepsilon, \quad (3)$$

where strains were small and the materials were linearly elastic ($\varepsilon \leq 0.01$). Strain rates (ε') were determined from elongation rate (v) and initial length,

$$\varepsilon' = v/L \quad (4)$$

Component Stresses and Strains

As load is applied, bimaterial composites deform with the same average stress in each component,

$$\sigma = \sigma_1 = \sigma_2. \quad (5)$$

*Corresponding author. Email: chuck_extrand@entegris.com

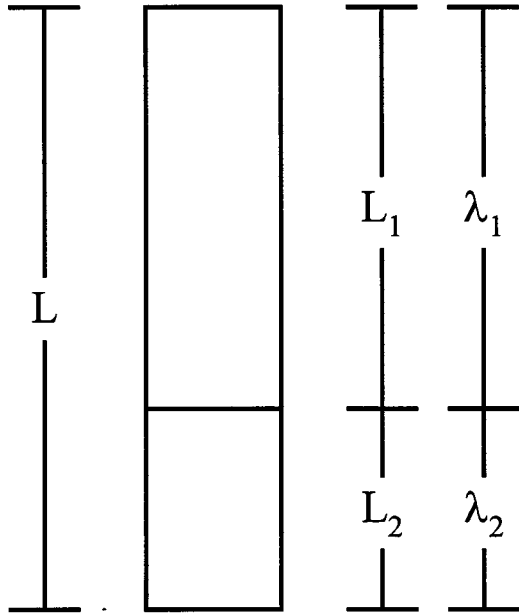


Fig. 1. A composite tensile specimen comprising two materials with different tensile moduli, E_1 and E_2 , where $E_1 \leq E_2$.

However, if the materials of construction differ in their stiffness, the individual components will not deform to the same extent. The stiffer material deforms less while softer material deforms more. The total change in length (L) is the sum of the change in each component,

$$\Delta L = \Delta L_1 + \Delta L_2 \quad (6)$$

The apparent strain (ϵ) in the composite sample is the sum of the strain in each of the components,

$$\epsilon = \Delta L/L = \lambda_1 \epsilon_1 + (1 - \lambda_1) \epsilon_2, \quad (7)$$

where

$$\lambda_1 = L_1/L, \quad (8)$$

$$\lambda_2 = L_2/L, \quad (9)$$

$$\epsilon_1 = \Delta L_1/L_1, \quad (10)$$

$$\epsilon_2 = \Delta L_2/L_2, \quad (11)$$

and

$$\lambda_1 + \lambda_2 = 1. \quad (12)$$

For $\lambda_1 = 1$, $L = L_1$. Conversely, for $\lambda_1 = 0$, $L = L_2$ (from Eqs 9 and 12).

The strain in each of the components is related to the applied stress via their respective tensile moduli,

$$\sigma_1 = E_1 \epsilon_1 \quad (13)$$

and

$$\sigma_2 = E_2 \epsilon_2. \quad (14)$$

Combining Eqs 5, 7, 13, and 14 gives the strain in each component in terms of apparent strain, component moduli, and component fraction,

$$\epsilon_1 = \epsilon / [\lambda_1 + (1 - \lambda_1) E_1 / E_2] \quad (15)$$

and

$$\epsilon_2 = \epsilon / [\lambda_1 E_2 / E_1 + (1 - \lambda_1)]. \quad (16)$$

Combining Eqs 5, 13, and 15, gives the apparent stress in series specimens in terms of apparent strain, component modulus, and fractional length,

$$\sigma = \{E_1 E_2 / [\lambda_1 E_2 + (1 - \lambda_1) E_1]\} \epsilon. \quad (17)$$

Apparent modulus of a series composite. From Eq 17, the apparent modulus (E) of a series composite tensile specimen is (15)

$$E = E_1 E_2 / [\lambda_1 E_2 + (1 - \lambda_1) E_1]. \quad (18)$$

Component Strain Rates and Deformation Speeds

Similar to strains, strain rates and deformation speeds of the composites depend on moduli of the components and their fractional length. Strain rates of the individual components are given by

$$\epsilon'_1 = \epsilon' / [\lambda_1 + (1 - \lambda_1) E_1 / E_2] \quad (19)$$

and

$$\epsilon'_2 = \epsilon' / [\lambda_1 E_2 / E_1 + (1 - \lambda_1)]. \quad (20)$$

Deformation speeds of the components (v_1 and v_2) differ from the apparent elongation rate (v) and can be calculated as

$$v_1 = \lambda_1 v / [\lambda_1 + (1 - \lambda_1) E_1 / E_2] \quad (21)$$

and

$$v_2 = (1 - \lambda_1) v / [\lambda_1 E_2 / E_1 + (1 - \lambda_1)]. \quad (22)$$

The limiting cases of $E_1 = E_2$ and $E_1 \ll E_2$ are discussed in the following section.

Limiting Cases

$E_1 = E_2$. If the moduli of the two segments are equal, then Eq 15 reduces to

$$\epsilon = \epsilon_1 \quad (23)$$

and Eq 17 to

$$\sigma = E_1 \epsilon. \quad (24)$$

Subsequently,

$$\sigma = E \epsilon = E_1 \epsilon_1. \quad (25)$$

$E_1 \ll E_2$. If the modulus of one segment is much greater than the other, then all deformation takes place in the softer segment. The relative strain in each component can be determined by combining Eqs 13 and 14,

$$\epsilon_2 = (E_1 / E_2) \epsilon_1. \quad (26)$$

Table 1. Tensile Properties of the Individual Materials.

Material	σ_y (MPa)	ϵ_y (m/m)	σ_b (MPa)	ϵ_b (m/m)	E (GPa)
C fiber PEEK	NY	NY	108 ± 1	0.017 ± 0.001	11.9 ± 0.3
PEEK	96 ± 1	0.025 ± 0.002	80 ± 3	0.16 ± 0.06	3.9 ± 0.2
PEI	109 ± 1	0.070 ± 0.001	93 ± 4	0.59 ± 0.06	3.3 ± 0.1
PBT	51 ± 1	0.031 ± 0.001	44 ± 2	2.4 ± 0.3	2.5 ± 0.1
PC	61 ± 1	0.060 ± 0.001	66 ± 1	1.0 ± 0.1	2.4 ± 0.1
PU	36 ± 1	0.043 ± 0.006	51 ± 1	3.3 ± 0.1	1.6 ± 0.1

NY: No yield.

If $E_1 \ll E_2$, Eq 26 reduces to

$$\epsilon_2 = 0, \quad (27)$$

Eq 15 reduces to

$$\epsilon = \lambda_1 \epsilon_1, \quad (28)$$

and Eq 17 reduces to

$$\sigma = (E_1/\lambda_1)\epsilon. \quad (29)$$

By combining Eqs 28 and 29, it can be shown that the apparent stress-strain behavior is determined by the much softer material,

$$\sigma = E\epsilon = (E_1/\lambda_1)\lambda_1\epsilon_1 = E_1\epsilon_1. \quad (30)$$

MATERIALS AND PROCEDURE

Materials

The following materials were used: polyetheretherketone (PEEK), C fiber PEEK, polyetherimide (PEI), polybutylene terephthalate (PBT), polycarbonate (PC), and a Shore A 55 durometer polyurethane (PU). The C fiber PEEK compound contained < 20% short C fiber.

Sample Preparation

Bimaterial composite samples were made by first molding dogbone-shaped tensile specimens (ASTM D638 Type 1), cutting them with a bandsaw, inserting a piece back into the mold, and then injecting another material. The bonding surface of several pre-molded specimens was polished with abrasive paper, but this treatment did not affect their strength.

Tensile Testing

Specimens were tested in tension at room temperature using an Instron® 5582 test machine equipped with a 100 kN static load cell and an extensometer (ASTM D638). Gauge length of the test machine was set at 115 mm. Bimaterial composite specimens were clamped such that the interface was equidistant from each clamp. The position of the extensometer was varied to give $\lambda_1 = 0.25, 0.50, \text{ or } 0.75$. (See Fig. 1.) Alternatively, λ_1 was varied by changing the position of the interface relative to the clamps.

Most samples were pulled at $v = 5 \text{ mm/min}$ ($\epsilon' = 8 \times 10^{-4} \text{ s}^{-1}$). A few monolithic specimens were tested at

other speeds to determine rate dependence of the materials. Five specimens of each monolithic/composite type were analyzed for yield stress, yield strain, breaking stress, breaking strain, and modulus; averages and standard deviations were calculated.

RESULTS AND DISCUSSION

Individual Components

The mechanical properties of the individual materials are summarized in Table 1. In general, agreement with literature values was excellent (16, 17). With the exception of the C fiber PEEK, all monolithic specimens yielded. Yield strains were small (2–7%) and similar in magnitude. The breaking strains of the unfilled samples varied more widely, from 16% for PEEK to more than 300% for PU. C fiber PEEK was the stiffest of the materials tested, about 3X stiffer than unfilled PEEK. The elastomeric PU was the softest. None of these materials exhibited appreciable rate dependence for the test speeds employed here. Strains and moduli remained constant up to $v = 50 \text{ mm/min}$ ($\epsilon' = 8 \times 10^{-3} \text{ s}^{-1}$). With this in mind, all composite specimens were tested at a single speed, $v = 5 \text{ mm/min}$. If materials were rate dependent, equivalent speeds and strains rates for monolithic and composite specimens could have been employed, Eqs 19–22.

Stress-Strain Behavior of Bimaterial Composites

Figure 2 shows typical stress-strain behavior of a PC/C fiber PEEK composite with the extensometer centered around the interface ($\lambda_1 = 0.50$). Stresses increased linearly with elongation and the samples broke at small apparent strains without yielding. Failure occurred at or near the interface with transfer of material from one component to the other, suggesting good adhesion. Other composite samples behaved similarly.

Effect of Relative Component Length

Stresses and Strains. By changing extensometer position, it was possible to test composites with a wide range of relative compositions. Figure 3 shows breaking stresses for PC composites with different fraction lengths (λ_1) of PC. The points are experimental data. Even though the relative length of PC varies, as expected, stresses were constant, Eq 5. The solid lines

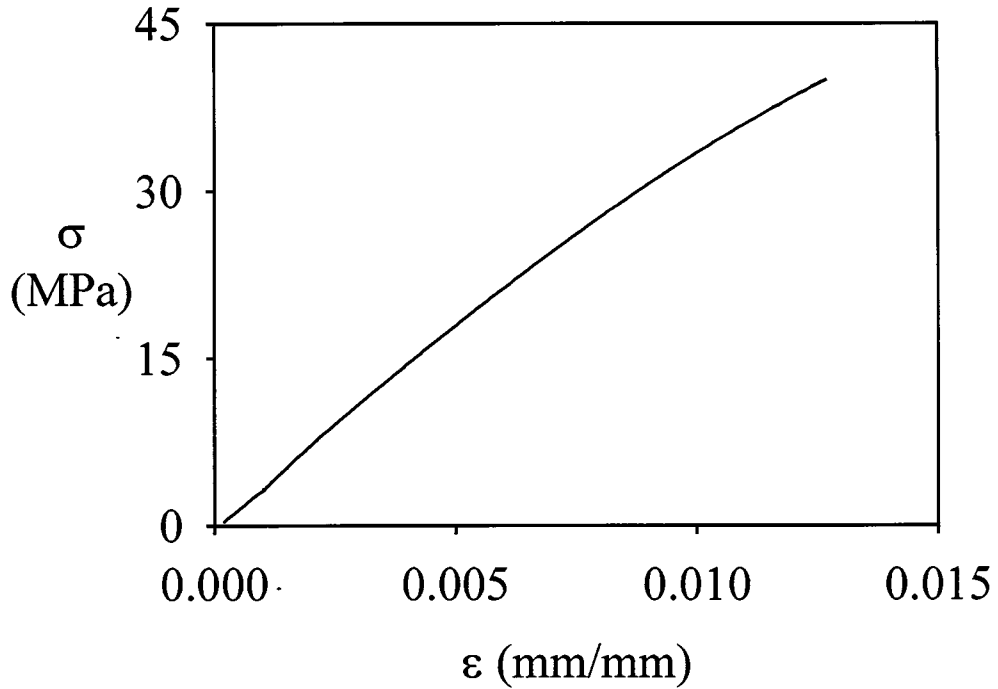


Fig. 2. Stress versus strain for a PC/C fiber PEEK sample with $\lambda_1 = 0.5$.

represent average values (40 ± 12 MPa for C fiber PEEK and 23 ± 9 MPa for PEEK). Other composite samples behaved similarly.

Figure 4 shows breaking strain (ϵ_b) versus fractional length of PC (λ_1) for several composites. Points are experimental data. The moduli of the C fiber PEEK and

unfilled PEEK are much greater than the moduli of PC. As a result, strains were not uniform throughout the specimens—the softer PC deformed more than its stiffer counterpart. Consequently, shifting extensometer position to increase the relative proportion of PC ($\lambda_1 \rightarrow 1$) increased the breaking strain. As expected

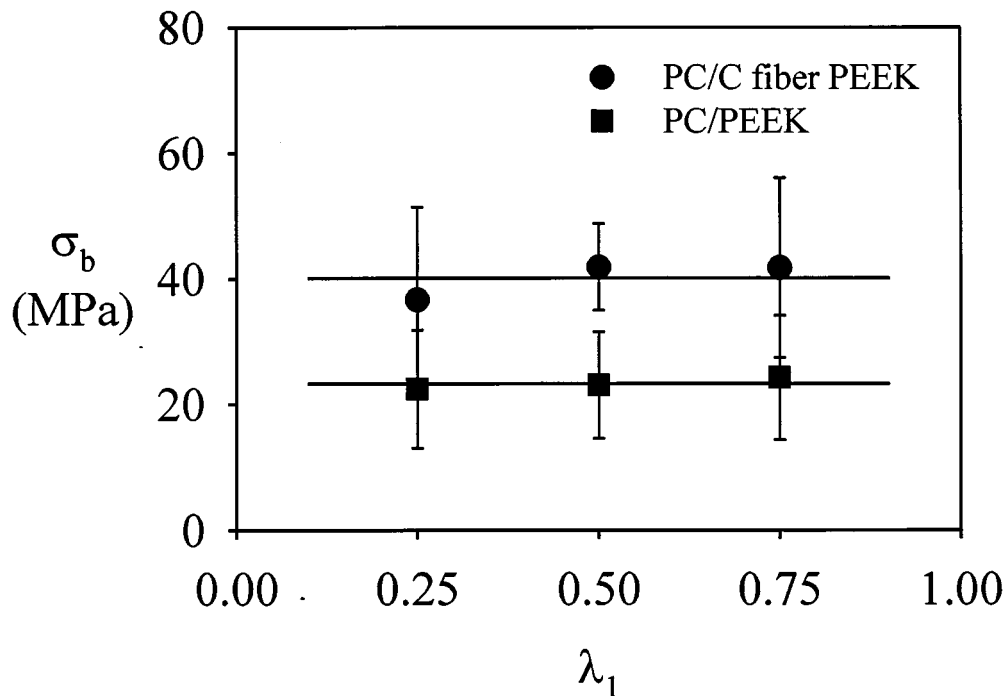


Fig. 3. Breaking stress (σ_b) versus fractional length of PC (λ_1). Points are experimental data; the solid lines represent average values.

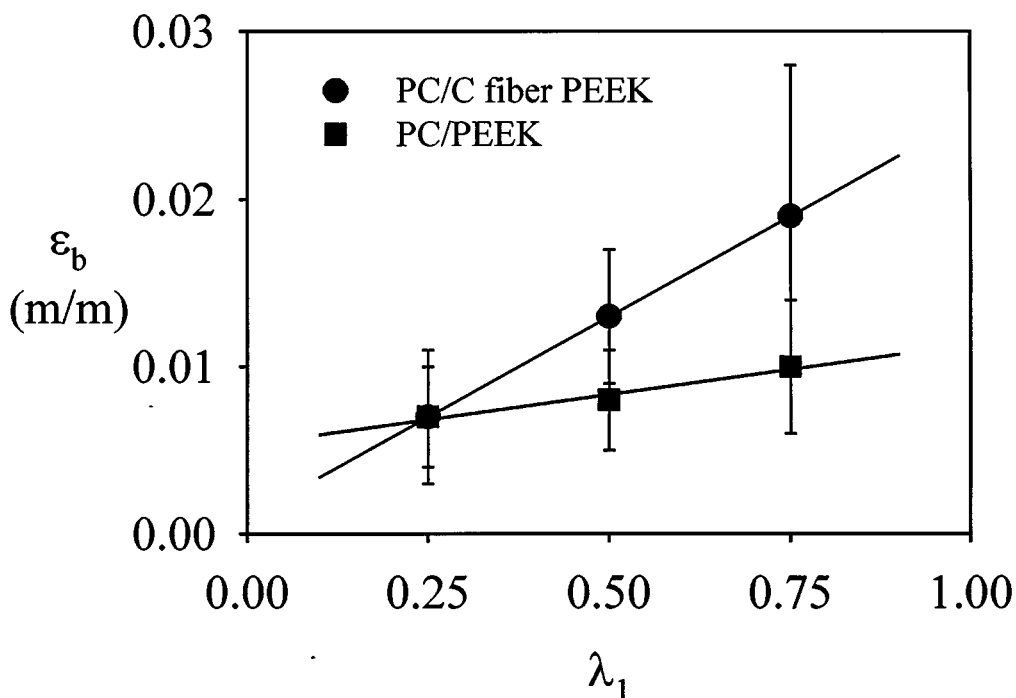


Fig. 4. Breaking strain (ϵ_b) versus fractional length of PC (λ_1). Points are experimental data; the solid lines represent linear regression.

from Eq 7, changes in apparent breaking strain were linear with relative component length. The slope is greater for the PC/C fiber PEEK composites than the PC/PEEK composites due to the greater difference in moduli. Slopes, intercepts, and regression coefficients from Fig. 4 are listed in Table 2.

Equation 7 accurately describes the apparent strain during elongation and correctly predicts a linear change in breaking strain with changes in λ_1 , but it cannot be used to estimate absolute values of the ultimate properties of the materials of construction. Note that breaking strains (and stresses) are much lower for the composite specimens than their monolithic counterparts. It is well known that an interface can act as flaw or stress raiser. The interface of the PC/PC composite demonstrates this effect quite well. Although the modulus of the PC composite was equal to the monolithic PC, the presence of an interface greatly reduced its strength. The PC/PC composite failed without yielding at 33 MPa, a 50% reduction in breaking stress. The interface also greatly reduced breaking strain—from 100% to less than 2%. Consequently, the breaking strain of the PC/PC specimen was similar to the other PC composites.

Moduli. Figure 5 shows the apparent moduli for several types of PC composites where the fractional length of the PC segment (λ_1) has been varied. The points are experimental data. Points at $\lambda_1 = 0$ represent monolithic C fiber PEEK or PEEK; points at $\lambda_1 = 1$ are for monolithic PC. The moduli of the composites were intermediate to the moduli of the individual components, decreasing with PC fraction. Solid lines were

calculated according to Eq 18. Agreement between measured and predicted values was excellent for both composite and monolithic specimens. The modulus of a PC/PC composite has been included for reference. Not surprisingly, the modulus of the PC/PC composite with the extensometer centered around its interface is the same as the monolithic PC.

Values of λ_1 also were varied by changing the clamp position, rather than extensometer position. For a given λ_1 value, modulus was not effected by changes in clamp position. However, changes in clamp position altered specimen compliance and consequently, influenced breaking stresses and breaking strains. (Ultimate (or fracture) properties depend upon specimen compliance and its effective flaw size (18). See, for example, refs. 4, 5.)

Various Composites

Table 3 summarizes the breaking stresses, breaking strains and tensile moduli of all composite samples tested with $\lambda_1 = 0.50$. All PC composites exhibited similar breaking strains. As mentioned previously,

Table 2. Slopes, Intercepts, and Regression Correlation for Breaking Strain (ϵ_b) Versus Component Fraction (λ_1), Figure 4.

material	intercept (10^{-3} m/m)	slope (10^{-3} m/m)	correlation (r^2)
PC/C fiber PEEK	1.0	24	1.000
PC/PEEK	5.3	6.0	0.9643

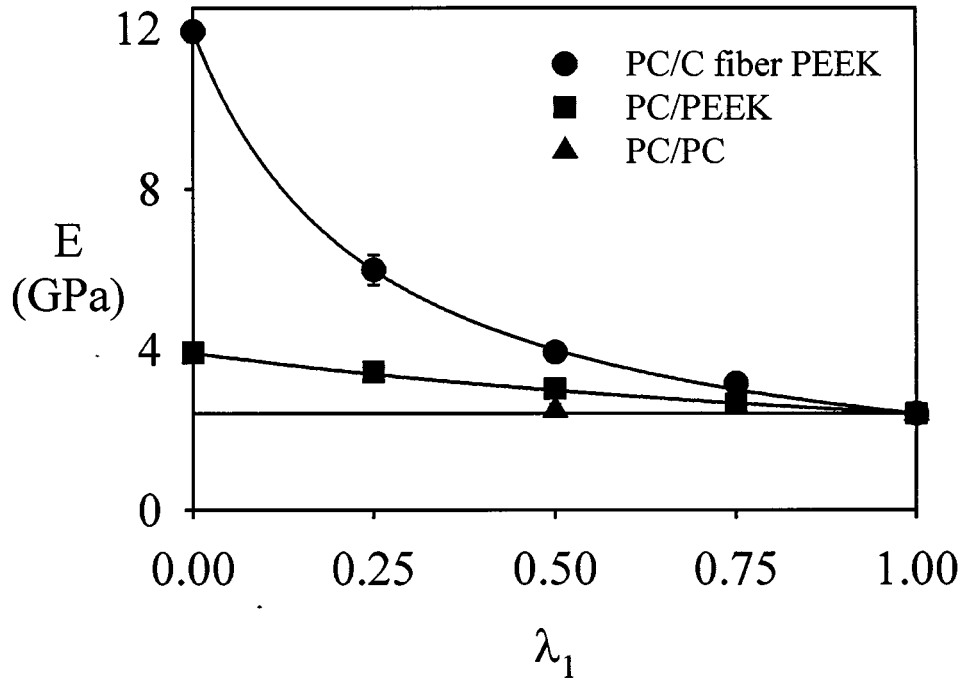


Fig. 5. Apparent tensile modulus (E) versus fractional length of PC (λ_1). The points are experimental data. Points at $\lambda_1 = 0$ represent monolithic PEEK or C fiber PEEK; points at $\lambda_1 = 1$ are for monolithic PC. Solid lines were calculated according to Equation 18.

failure occurred near the specimen interface usually accompanied by transfer of material from one component to the other. PEI and PEEK showed minimal material transfer.

For $\lambda_1 = 0.50$, Eq 18 can be rewritten in a reduced form,

$$E/E_1 = 2E_2/(1 + E_2/E_1). \quad (31)$$

The moduli of all PC composites with $\lambda_1 = 0.50$ are shown graphically in Fig. 6 according to Eq 31. The points are experimental data. The solid line represents the predicted behavior; agreement was excellent.

Limiting Cases

$E_1 = E_2$. The PC/PC composite represents the limiting case where the moduli of the two components were equal. Accordingly, the apparent modulus of the PC/PC composite was equal to the modulus of the monolithic PC, Eqs 23–25.

$E_1 \ll E_2$. PU/C fiber PEEK composites represent the case where one component was much stiffer than the other. Here, $E_{\text{C fiber PEEK}}/E_{\text{PU}} = 7.5$. Nearly all deformation took place in the softer PU segment and the apparent modulus of the composite was equal to that of monolithic PU, about 1.5 GPa, Eqs 26–30.

CONCLUSIONS

Stresses of the bimaterial composites increased linearly with elongation and the samples broke at small apparent strains without yielding. Breaking stresses and strains of the composites were less than those of the individual components. Failure occurred at or near the interface with transfer of material from one component to the other, suggesting good adhesion. For any given bimaterial composite, breaking stresses were independent of fractional length. On the other hand, both elongation to break and apparent stiffness varied with fractional length.

Table 3. Tensile Properties of Various Composite Samples with Extensometer Centered Around Interface ($\lambda_1 = 0.5$, $v = 5\text{mm/min}$, 25°C).

Composite	σ_b (MPa)	ϵ_b (m/m)	E (MPa)
C fiber PEEK on PC	42 ± 7	0.013 ± 0.004	3.9 ± 0.1
PEEK on PC	29 ± 9	0.011 ± 0.004	3.1 ± 0.2
PEI on PC	30 ± 4	0.011 ± 0.002	3.3 ± 0.5
PBT on PC	33 ± 9	0.015 ± 0.006	2.6 ± 0.1
PC on PC	33 ± 14	0.017 ± 0.009	2.5 ± 0.1
C fiber PEEK on PU	6 ± 3	0.005 ± 0.003	1.4 ± 0.2

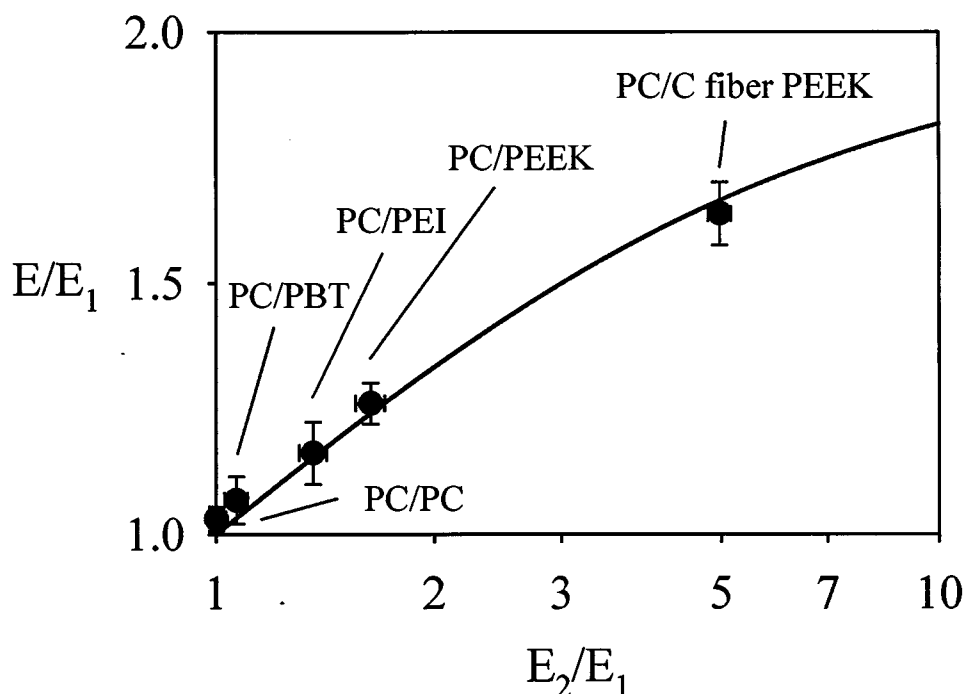


Fig. 6. Relation between the apparent modulus and moduli of the individual components for $\lambda_1 = 0.50$. The points were calculated from experimental data, Tables 1 and 3; the solid line was calculated from Equation 31.

ACKNOWLEDGMENTS

The authors wish to thank Entegris management for allowing the publication of this work. Also, thanks to G. Smith and T. Raser for molding of the test specimens, as well as R. Kariniemi and J. McPhee for assistance in the mechanical testing.

REFERENCES

1. J. De Gaspari, *Plastics Technology*, **44**, 44 (1992).
2. H. H. Kausch, *Advanced Thermoplastic Composites*, Hanser Publishers, New York (1993).
3. C. W. Extrand and S. Bhatt, *J. Appl. Polym. Sci.*, **76**, 1777 (2000).
4. C. W. Extrand and S. Bhatt, *J. Adhesion*, **72**, 219 (2000).
5. C. W. Extrand and S. Bhatt, *J. Mat. Sci.*, **35**, 5427 (2000).
6. M. L. Williams, *Bull. Seism. Soc. Am.*, **49**, 199 (1959).
7. G. C. Sih and J. R. Rice, *J. Appl. Mech.*, **31**, 477 (1964).
8. F. Erdogan, *J. Appl. Mech.*, **32**, 403 (1965).
9. J. R. Rice and G. C. Sih, *J. Appl. Mech.*, **32**, 418 (1965).
10. V. L. Hein and F. Erdogan, *Int. J. Fracture Mech.*, **7**, 317 (1971).
11. G. P. Anderson, S. J. Bennett, and K. L. DeVries, *Analysis and Testing of Adhesive Bonds*, Academic Press, New York (1977).
12. S. Wu, *Polymer Interface and Adhesion*, Marcel Dekker, New York (1982).
13. I. M. Ward, *Mechanical Properties of Solid Polymers*, 2nd Edition, John Wiley, New York (1983).
14. J. M. Gere and S. P. Timoshenko, *Mechanics of Materials*, 2nd Edition, PWS-Kent Publishing Co., Boston (1984).
15. L. E. Nielsen and R. F. Landel, *Mechanical Properties of Polymers and Composites*, 2nd Edition, Marcel Dekker, New York (1994).
16. H. Saechtling, *International Plastics Handbook*, 2nd Edition, Oxford University Press, New York (1987).
17. *International Plastics Selector*, Edition 17, Volume 2, D.A.T.A. Business Publishing, Englewood, Colo. (1996).
18. J. G. Williams, *Fracture Mechanics of Polymers*, Wiley, New York (1987).